Antiferromagnetic structure of UNiAl

K. Prokeš*
Van der Waals–Zeeman Institute, University of Amsterdam, 1018 XE Amsterdam, The Netherlands

F. Bourdarot, P. Burlet, P. Javorský,† and M. Olšovec†
CENG-CEA, DRFMC-SPSMS-MDN, 38054 Grenoble Cedex 9, France

V. Sechovský
Department of Metal Physics, Charles University, Ke Karlovu 5, 121 16 Prague 2, The Czech Republic

E. Brück, F. R. de Boer, and A. A. Menovsky
Van der Waals–Zeeman Institute, University of Amsterdam, 1018 XE Amsterdam, The Netherlands
(Received 13 January 1998; revised manuscript received 5 March 1998)

UNiAl crystallizes in the hexagonal ZrNiAl-type structure. Magnetic, transport, and thermal properties of UNiAl point to an antiferromagnetic (AF) ordering below $T_N = 19.3$ K. Below this temperature UNiAl orders with propagation vector $\mathbf{q} = (0.1,0.1,0.5)$. U magnetic moments are oriented along the hexagonal axis and modulated sinusoidally within the basal plane. The modulation is not even partially squared-up down to 1.7 K. The maximum size of U moment is $(1.24 \pm 0.03)\mu_B$/U. However, the three U atoms that are crystallographically equivalent do not carry the same moment within the crystallographic unit cell. The propagation vector of AF structure does not change in the whole temperature range. AF correlations that propagate also with $\mathbf{q} = (0.1,0.1,0.5)$ can be traced at temperatures up to 30 K showing the critical scattering near T_N.
[S0163-1829(98)02529-6]

I. INTRODUCTION

Compounds containing $5f$-electron states have been the subject of intensive experimental and theoretical studies over past few decades due to numerous different ground states. Systematic studies of equiatomic UTX (T, late transition metal; X, p-electron element) compounds crystallizing in several distinct crystal structures[1,2] revealed that the magnetocrystalline anisotropy is closely related to the anisotropy in the bonding of $5f$ electrons. In this respect, one deals with hybridization-induced magnetocrystalline anisotropy. The degree of hybridization depends on the relative position of d and $5f$ bands within the energy scale. The most pronounced consequence of hybridization is delocalization of $5f$-electron states as the strength of hybridization increases. Consequently, the ground state can change within a certain isostructural group of compounds as a function of constituent T and/or X elements from Pauli paramagnetism through weak ferromagnetic or spin fluctuation behavior towards long-range magnetic order. This development is readily observed also in other U-based compounds[2,3] and is due to the gradual reduction of the $5f$-d hybridization on going from left to right (or from top to bottom) in the Periodic Table. As the $5f$ electronic states participate both in bonding and magnetism, we can expect a strong relation also between the transport and thermal properties on the one side and magnetic anisotropy on the other.

UNiAl is a member of the large group of ternary uranium compounds crystallizing in the hexagonal ZrNiAl-type structure.[1,2] The following conclusions were drawn from results of susceptibility, magnetization, specific-heat, and electrical-resistivity studies on UNiAl:[1] (a) antiferromagnetic (AF) ordering below $T_N = 19.3$ K, (b) uniaxial magnetic anisotropy in both AF and paramagnetic regions (c axis is an easy magnetization direction), (c) large negative (anisotropic) magnetoresistance effect due to a metamagnetic transition, (d) large value of the low-temperature specific-heat coefficient $\gamma \approx 167$ mJ/K^2 mol, which may be due to magnetic fluctuations in the ordered state, and (e) pronounced and anisotropic dependence of the specific heat and resistivity on an applied magnetic field.

Although UNiAl has been the subject of intensive studies already for a couple of years,[1,2,4,5] the details about the antiferromagnetic structure at low temperatures remained unclear, mainly due to lack of a good-quality single crystal in the past. Recently, a new, large, and good-quality single crystal grown by a modified Czochralski method has become available. This made our neutron studies at CENG-CEA Grenoble possible. Here we report results on elastic neutron-diffraction studies.

II. EXPERIMENTAL METHODS

A single crystal of UNiAl has been grown from a slightly off-stoichiometric melt (excess of U) by a modified tri-arc Czochralski technique in continuously gettered Ar atmosphere at the FOM-ALMOS center at the University of Amsterdam. In order to reduce mosaicity, the seed was tilted from the easy-grow direction by an angle of 15°. No subsequent heat treatment was given to the as-cast ingot. The quality of the resulting product was checked by x-ray diffraction and by electron microprobe analysis (EPMA). It has been found to be single crystalline and homogeneous with composition deviating from the ideal stoichiometry by no more

than 1 at. % (resolution limit of EPMA). The cylindrical-shape part (0.4 g) of this single crystal was sparked-out and used in the neutron-diffraction experiments.

The integrated intensities were measured on the DN3 normal beam diffractometer at the SILOE reactor at CENG-CEA, Grenoble in two subsequent experiments. In the first one, the crystal was mounted with its hexagonal axis perpendicular to the rotational axis of the diffractometer. In this configuration, we could reach nuclear and magnetic (hkl) reflections with high l index. In the second experiment, the same crystal was mounted with its c axis parallel to the rotational axis of the diffractometer. However, in this experiment we could not reach (hkl) reflections with l index higher than 1. In both cases, the crystal was encapsulated in a small aluminum container, sealed under helium, and measured with an incident-neutron wavelength of 1.541 Å. The DN3 diffractometer is equipped with a single, lifting-counter detector and $\lambda/2$ contamination filter leaving residual contamination on the level of 5×10^{-4}.

In both experiments, the single crystal was oriented using several sufficiently strong and well-centered nuclear reflections. The cell parameters were refined from the UB matrix and the scan profiles were analyzed by the Lehman-Larson algorithm.[6]

The crystallographic and magnetic structures were determined by fitting procedures using the programs GSAS (Ref. 7) and FULLPROF.[8] The function minimized during least-squares refinement was $\Sigma w|F_{\rm obs}-F_{\rm calc}|^2$, $w=1/\sigma^2$. The scattering lengths were taken from Ref. 9 and the U^{3+} ($\langle j_0\rangle+c_2\langle j_2\rangle$) magnetic form factor from Ref. 10.

III. RESULTS

A. Crystal structure

Using 73 (32 inequivalent) reflections from the first experiment (c axis perpendicular to the rotational axis of the diffractometer) and 60 (29 inequivalent) reflections from the second experiment, both sets observed at 40 K, we confirmed that UNiAl forms in the hexagonal ZrNiAl-type structure (space group $P\bar{6}2m$). This structure (Fig. 1) is built up by alternating two types of basal plane atomic layers along the c axis. One of them contains the U atoms and $\frac{1}{3}$ of the Ni atoms. The other one consists of the rest of the Ni atoms together with Al atoms. Each U atom has four nearest U neighbors within the basal plane and two other neighbors along the c axis. Bonding of the U $5f$ states within the basal plane gives rise to a strong uniaxial magnetocrystalline anisotropy with the easy magnetization direction along the c axis.[1] For the crystal-structure refinement we have utilized the general structure analysis system (GSAS) because of its ability to refine two independent sets of observations simultaneously.

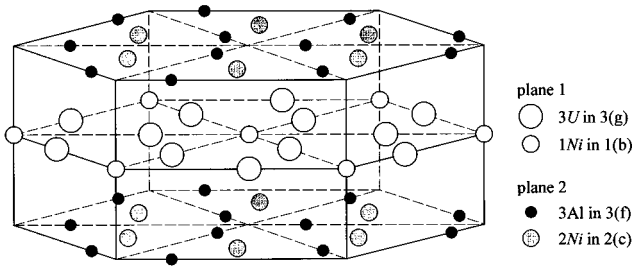

FIG. 1. Schematic representation of the crystal structure of UNiAl crystallizing in the hexagonal ZrNiAl type of structure.

Although the results of the fit that included absorption, scale factors, positions, and temperature factors of the atoms as free parameters were in good agreement with expected values, the factors referring to the quality of fit were not satisfactorily low. It is especially well known that extinction and stoichiometry (occupation of constituent elements) are the main obstacles in the single-crystal neutron-scattering experiment. Therefore we also included in the refinement the extinction parameters (Becker-Coppens model[11]) and the occupation numbers as free parameters. The best agreement between the fit and data was obtained by using the secondary extinction. The quality of the fit was not improved by inclusion of the primary extinction into the fit. The refined results suggest that the extinction is mostly caused by small mosaic spread of large domains. The results of this fit are summarized in Table I.

In addition, the quality of the fit was not improved when the occupation numbers were allowed to be free parameters. This means that the stoichiometry of our sample does not deviate significantly from the ideal 1:1:1 composition. This result is in good agreement with the electron-microprobe-analysis results.

B. Ground-state magnetic-structure determination

Previous neutron-diffraction experiments made on a powder sample[5] and on a single crystal[4] have indicated at 4.2 K an antiferromagnetic structure with $\mathbf{q}=\pm(0.1,0.1,0.5)$ and

TABLE I. Refined structural parameters for UNiAl at 40 K.

Structure type: ZrNiAl Space group: P-62m	Site	Local symmetry	Position parameters		B (Å^2) $T=40$ K
U	3(g)	($m2m$)	$x_{\rm U}\,0\,\frac{1}{2}$	$x_{\rm U}=0.5719(9)$	0.16(2)
Ni I	1(b)	($-62m$)	$0\,0\,\frac{1}{2}$		0.10(1)
Ni II	2(c)	(-6)	$\frac{1}{3}\,\frac{2}{3}\,0$		0.18(2)
Al	3(f)	($m2m$)	$x_{\rm Al}\,0\,0$	$x_{\rm Al}=0.2306(19)$	0.34(5)
Cell parameters: $a=669.2\pm0.8$ pm, $c=401.0\pm0.7$ pm					
Maximal extinction: 0.61					
R factors: $R=3.24\%$, $\chi^2=5.38$					

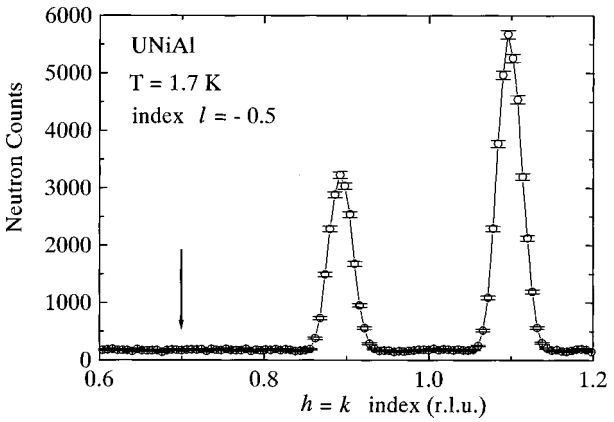

FIG. 2. Representative reciprocal scan along the [110] direction at 1.7 K. Clearly, additional magnetic Bragg reflections can be indexed using the propagation vector $\mathbf{q}=\pm(0.1,0.1,0.5)$. Note that no intensity is recorded around the $\pm(0.3,0.3,0.5)$ position marked by the arrow.

the U moments oriented along the *c* axis. Due to poor quality of the used single crystal, it was not possible to refine the magnetic structure of UNiAl.

As the temperature is lowered below the magnetic-phase-transition temperature $T_N=19.3$ K, additional Bragg peaks are observed. We assume these reflections to be of magnetic origin. In Fig. 2, we show a representative reciprocal scan along the [110] direction at 1.7 K. Clearly, we observe additional magnetic Bragg reflections that can be indexed using the propagation vector $\mathbf{q}=\pm(0.1,0.1,0.5)$. This result suggests antiferromagnetic coupling of the moments along the *c* axis and some kind of modulation within the basal plane. Since no additional intensity is recorded at the nuclear Bragg peaks, the net magnetic moment in each basal plane is zero. The fact that no diffracted intensity is recorded at $\pm(0.3,0.3,0.5)$ positions yields a sine-wave profile modulation of the U magnetic moments in the basal plane, i.e., no squaring-up of the in-plane modulation is observed down to 1.7 K.

In order to sort out all possible magnetic structures that are compatible with a paramagnetic crystal-structure space group and with the experimentally determined propagation vector, we have used irreducible representation theory as developed by Bertaut.[12] There are only four among the 12 symmetry operations within $P\bar{6}2m$ space group that leave the propagation vector $\mathbf{q}=\pm(0.1,0.1,0.5)$ invariant: the identity *E*, a mirror plane perpendicular to the *c* axis $m(x,y,0)$, a twofold rotation axis along the [110] direction $2(x,x,0)$, and a mirror plane containing this axis and the *c* axis $m(x,x,z)$. It is easy to check that these four elements commute with each other and form a group. Consequently, there are four one-dimensional irreducible representations. The effects of the symmetry elements on the U-moment components are listed in Table II. We note that there is no such symmetry operation that would project U atoms from the $(x_U,0,\frac{1}{2})$ (U_1) or the $(0,x_U,\frac{1}{2})$ (U_2) position to the $(-x_U,-x_U,\frac{1}{2})$ (U_3) position and it follows that these two U atomic positions are disconnected. Let us note, that we suppose, at this time, no magnetic moment at the transition-metal atom (Ni). This is a fairly reasonable assumption as the compounds YNiAl and LuNiAl that crystallize in the same hexagonal structure are nonmagnetic.[13] Therefore, only an induced magnetic moment on Ni atoms due to U moments can be expected as has been observed for instance, by Paixão *et al.* for isostructural URhAl:[14] We will restate this question in Sec. III C.

TABLE II. Symmetry operations on moment components in the crystallographic unit cell of UNiAl. Note that there is no mixing between atoms U_1 and U_2 on one side and atom U_3 on the other.

Moment components	Symmetric operations			
	$M(E)$	$M(m_{xy0})$	$M(2_{xx0})$	$M(m_{xxz})$
μ_{1x}	μ_{1x}	$-\mu_{1x}$	$-\mu_{2y}$	μ_{2y}
μ_{2x}	μ_{2x}	$-\mu_{2x}$	$-\mu_{1y}$	μ_{1y}
μ_{3x}	μ_{3x}	$-\mu_{3x}$	$-\mu_{3y}$	μ_{3y}
μ_{1y}	μ_{1y}	$-\mu_{1y}$	$-\mu_{2x}$	μ_{2x}
μ_{2y}	μ_{2y}	$-\mu_{2y}$	$-\mu_{1x}$	μ_{1x}
μ_{3y}	μ_{3y}	$-\mu_{3y}$	$-\mu_{3x}$	μ_{3x}
μ_{1z}	μ_{1z}	μ_{1z}	μ_{2z}	μ_{2z}
μ_{2z}	μ_{2z}	μ_{2z}	μ_{1z}	μ_{1z}
μ_{3z}	μ_{3z}	μ_{3z}	μ_{3z}	μ_{3z}

Basis vectors corresponding to each irreducible representation are obtained by the projection-operation method.[15] By combining the results obtained for both disconnected U positions belonging to the same irreducible representation, magnetic models are derived. It follows that the magnetic moments on all U sites can be either along the hexagonal *c* axis or perpendicular to it (Table III). There are four basic magnetic-structure models associated with the propagation vector $\mathbf{q}=\pm(0.1,0.1,0.5)$ represented in Fig. 3. In models *A* and *B*, the U moments orient along the hexagonal axis; however, these models differ significantly. In model *A*, all the moments within one crystallographic unit cell are coupled ferromagnetically. In model *B*, the two connected U moments are coupled antiferromagnetically and the disconnected one has to be zero. In models *C* and *D*, the U moments lie within the basal plane.

TABLE III. Possible U magnetic moment configurations in UNiAl.

Model	Moment components								
	μ_{1x}	μ_{2x}	μ_{3x}	μ_{1y}	μ_{2y}	μ_{3y}	μ_{1z}	μ_{2z}	μ_{3z}
A	0	0	0	0	0	0	μ_{2z}	μ_{1z}	μ_{3z}
B	0	0	0	0	0	0	$-\mu_{2z}$	$-\mu_{1z}$	0
C	$-\mu_{2y}$	$-\mu_{1y}$	$-\mu_{3y}$	$-\mu_{2x}$	$-\mu_{1x}$	$-\mu_{3x}$	0	0	0
D	μ_{2y}	μ_{1y}	μ_{3y}	μ_{2x}	μ_{1x}	μ_{3x}	0	0	0

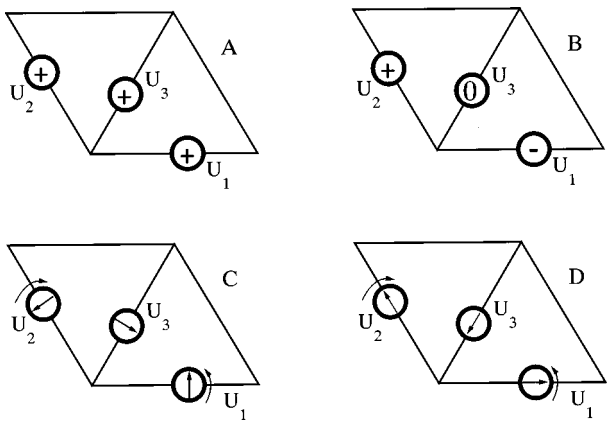

FIG. 3. Possible magnetic structures of UNiAl considering only U moments derived by group analysis for propagation vector $\pm(0.1,0.1,0.5)$ within one U-Ni basal plane. U moments in the next U-Ni layer are coupled antiferromagnetically to moments shown in the figure. Symbols in circles denote magnetic moment oriented parallel to the c axis (+), magnetic moment oriented antiparallel to the c axis (−), and no moment allowed (0).

One propagation vector would mean that with each nuclear Bragg peak only one pair of magnetic peaks is associated. However, six magnetic reflections are associated with each nuclear Bragg peak, in three pairs. Here we are dealing with a hexagonal system, so there are other propagation vectors, $\mathbf{q}'=\pm(-0.1,0.2,0.5)$ and $\mathbf{q}''=\pm(-0.2,0.1,0.5)$ that are symmetrically equivalent to $\mathbf{q}$. One has to be careful with the fact that $\mathbf{q}$ ends at the Brillouin-zone boundary because then, in some cases, the propagation vector $\mathbf{q}$ does not need to be associated with $-\mathbf{q}$. However, in our case, it is necessary to associate with each of the propagation vectors $\mathbf{q}$, $\mathbf{q}'$, or $\mathbf{q}''$ also $-\mathbf{q}$ directions to index all reflections and to make magnetic moments a real quantity. For instance, the reflection (0.9,0.9,0.5), can be indexed as $(1,1,1)^{-\mathbf{q}}$ and the reflection (1.1,0.8,0.5) as $(1,1,1)^{-\mathbf{q}'}$.

Then the question arises whether the magnetic structure is characterized by all three $\mathbf{q}$ vectors (triple-$\mathbf{q}$ structure), if it contains three domains, each of them characterized by one $\pm\mathbf{q}$ vector (single-$\mathbf{q}$ structure), or if it mixes both (three domains of triple-$\mathbf{q}$ or double-$\mathbf{q}$ structures). We have to consider the fact that the crystallographic unit cell contains three magnetic moments that do not necessarily propagate with the same propagation vector. From this point of view, there are three possibilities: (a) each of the three U magnetic moments propagates with different propagation vector (this would correspond to triple-$\mathbf{q}$ structure), (b) all of them propagate with the same propagation vector (single-$\mathbf{q}$ structure), for (c) magnetic moments at connected positions $(x,0,\frac{1}{2})$ and $(0,x,\frac{1}{2})$ propagate with the same propagation vector and the moment at the remaining position $(-x,-x,\frac{1}{2})$ propagates with one of the remaining propagation vectors (double-$\mathbf{q}$ structure).

It is well known[15] that it is not possible to distinguish between multiple-$\mathbf{q}$ structures and single-$\mathbf{q}$ structures with magnetic domains that are equally populated, which is the situation normally encountered in zero magnetic field. Both structures give the same integrated intensities for equivalent magnetic reflections. This is not true if a crystallographic distortion takes place at the magnetic phase transition that lowers the symmetry of the structure leading to preferential population of one magnetic domain. However, our data do not indicate within the given resolution of the diffractometer the presence of any distortion. The other possibility to solve the problem would be the application of a magnetic field, application of the uniaxial stress on the single-crystalline sample, or using high-resolution neutron powder or x-ray diffractometers at low temperatures.

We do see a statistically significant difference between the integrated intensities of the six magnetic reflections around the origin of the reciprocal space that are equivalent from the point of view of the geometry of the experiment. Therefore, we conclude that UNiAl contains three magnetic domains.

In total, 164 magnetic reflections in both (c parallel and perpendicular to the rotational axis of the diffractometer) experiments were measured. For the magnetic-structure refinement, only the magnetic reflections for which $I>3\sigma(I)$ were selected (96 reflections). The results of the fits to the models depicted in Fig. 3 are summarized in Table IV. As can easily be seen, the best agreement is achieved for model A in which the two disconnected U positions carry different moments (i.e., $\mu_{U_1}=\mu_{U_2}\neq\mu_{U_3}$). The six magnetic reflections for each nuclear reflection were generated by three magnetic domains. By different combinations of the propagation vectors assigned to these magnetic domains and two disconnected U positions it became clear that the only consequence is a different μ_{U_1}/μ_{U_3} ratio for differently populated magnetic domains. It seems to be quite reasonable to suppose the same μ_{U_1}/μ_{U_3} ratio for all three magnetic domains that is achieved in the case of a single-$\mathbf{q}$ magnetic structure (i.e., within each magnetic domain there is only one propagation vector for all U positions). We found the three magnetic domains populated with the ratio 31.7%:27.4%:40.9%.

TABLE IV. Results of the fits to different magnetic-structure models of UNiAl depicted in Fig. 3 F denotes fixed parameter, φ and ϑ are angles between moment μ_U and the a axis and the c axis, respectively.

Model	μ_{U_1,U_2} (μ_B)	φ (deg)	ϑ (deg)	μ_{U_3} (μ_B)	φ (deg)	ϑ (deg)	μ_{U_1}/μ_{U_3}	μ_{mean} (μ_B)	χ^2
A	1.24 (3)	0 (F)	0 (F)	0.54 (9)	0 (F)	0 (F)	0.44	0.64 (3)	7.10
A_{eq}	1.08 (4)	0 (F)	0 (F)	1.08 (4)	0 (F)	0 (F)	1.00	0.69 (2)	25.6
B	0.58 (18)	0 (F)	0 (F)	0 (F)	0 (F)	0 (F)	0	0.25 (7)	183
C	0.77 (16)	−36.1 (8)	90 (F)	0.93 (29)	−30 (F)	90 (F)	1.21	0.52 (14)	124
D	0.65 (15)	59.5 (8)	90 (F)	0.74 (26)	60 (F)	90 (F)	1.14	0.43 (12)	123

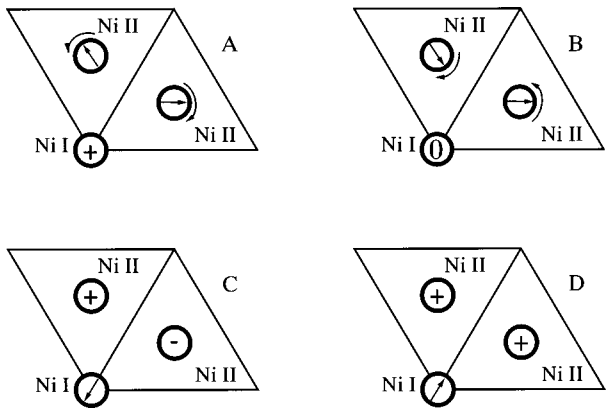

FIG. 4. Possible Ni moment configurations in UNiAl derived by group analysis for propagation vector $\pm(0.1,0.1,0.5)$ projected to the basal plane. Ni moments in the next layer are coupled antiferromagnetically to moments shown in the figure.

These values are close to $\frac{1}{3}$, a value to be found in the case of equally populated domains. However, at the same time the population of the domains differs enough to explain the differences in the integrated intensities of the geometrically equivalent magnetic reflections around the origin of the reciprocal space. Let us note that the difference in magnitude of the U moments μ_{U_1} and μ_{U_3} on disconnected positions is important. This is demonstrated by the fit to the model denoted in Table IV as A_{eq} that differs from model A only by the fact that all U magnetic moments are equal. This fit yields an almost identical magnetic domain population that is about a 20% smaller magnitude of μ_{U_1}. However, the χ^2 value increases by more than a factor of 3. The other models B, C, and D yield a very bad agreement with experimental observations.

C. Nonzero Ni magnetic moments

Up to now, we have supposed no magnetic moment at Ni positions. However, small induced moments can be expected due to hybridization between $3d$ and $5f$ states.[14] Possible configurations of the Ni moments compatible with the space group and the propagation vector **q** were derived in the very same manner as for U moments. In this case, two inequivalent Ni sites [$1(b)$ and $2(c)$] have to be treated independently. The possible moment configurations are depicted in Fig. 4. There are four models corresponding to four one-dimensional representations. They are labeled in the same way as in the case of U moments. As can be seen, the moment on Ni I at position $1(b)$ that is situated in the U basal plane is within the A model oriented along the c axis, i.e., it can be parallel or antiparallel to the U moments. The Ni II moments on the $2(c)$ position are oriented perpendicular to the hexagonal axis. In model B there cannot be any moment at the Ni I site and the moments at Ni II sites are within the basal plane. In models C and D, the moment on the Ni I site is within the basal plane and the moments on the Ni II sites are oriented along the hexagonal axis, coupled antiferromagnetically and ferromagnetically with each other, respectively.

The fits of the experimental data to all models yield the conclusion that the experimental data do not allow accurate determination of the magnitude of the Ni moments. The magnitude of Ni moments is in all cases very small and appears to be below the detection limit of the experiment. Considering all possible models allowed by symmetry we estimate the upper limit for the magnitude of Ni moments to be about $0.1\mu_B$/Ni. This implies negligible influence on the U moments, domain population, etc. and therefore also on the quality of the fits.

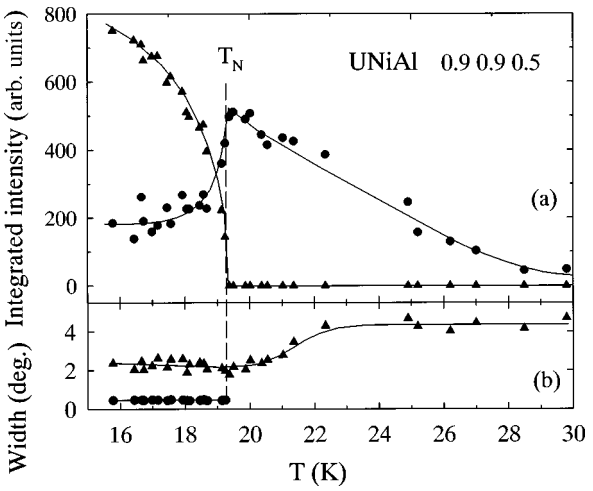

FIG. 5. Temperature dependence of the integrated intensity of both the magnetic (0.9,0.9,0.5) reflection (●) and the diffuse scattering around this position (▲) of UNiAl (a) and their width at half maximum (b). The lines are guides for eye.

D. Diffuse scattering

It is well known that the influence of magnetic fluctuations in the vicinity of the magnetic phase transition gives rise to additional magnetic-scattering intensity that can be recorded in a diffuse-scattering experiment. As has been shown by Brück *et al.*,[1] there are clear deviations from the expected temperature dependencies of some bulk properties that can be attributed to magnetic fluctuations in the vicinity of T_N. In Fig. 5, the temperature dependence of the integrated intensity [Fig. 5(a)] and width at the half-maximum [Fig. 5(b)] of both the magnetic (0.9,0.9,0.5) reflection and the diffuse scattering around this reflection are shown. As the temperature approaches the magnetic phase transition, broad diffuse scattering centered at (0.9,0.9,0.5) appears. Above T_N, the diffuse-scattering intensity increases with decreasing temperature. At the same time, the width of the Lorentz-shape diffuse-scattering peak decreases, reflecting that the spatial correlations increases [Fig. 5(b)]. Below T_N, the magnetic (0.9,0.9,0.5) reflection emerges on top of the diffuse scattering as a result of the onset of coherent scattering due to long-range magnetic order. Its width stays constant below T_N. Antiferromagnetic correlations can be traced at least up to 30 K, a temperature that is 50% higher than T_N. The onset of antiferromagnetic correlations clearly coincides with the change of the sign of the temperature derivative of the electrical resistivity. The electrical resistivity for both orientations (current parallel to the hexagonal axis and perpendicular to it) decreases slowly with lowering temperature; they reach broad minima at 30 K and form maxima at 18 K ($\rho \| c$) and 14 K ($\rho \perp c$), respectively. The increase of the electrical resistivity with lowering temperature was previ-

ously attributed to appearance of antiferromagnetic correlations and our results support this statement. It is interesting that the intensity of the diffuse scattering in the ordered region seems to be higher than in the paramagnetic state well above T_N, suggesting that magnetic fluctuations might be present even in the long-range antiferromagnetic state. Due to high magnetic anisotropy of this system, any deviations of the moment direction from the c axis are forbidden and therefore ordinary low-energy transverse spin waves are not favorable. In this case, when only the moment size is not fixed, the possibility of longitudinal fluctuations has to be considered. However, to clarify unambiguously the origin of the diffuse scattering an inelastic neutron-scattering experiment is highly desirable.

IV. DISCUSSION AND CONCLUSIONS

The electronic structure of actinides is characterized by partially occupied $5f$-electron states in analogy with partly occupied $4f$ states in lanthanides. However, there are fundamental differences between the character of the $4f$- and $5f$-electron states in metals. The most important one is a much larger spatial extent of the $5f$ wave functions, and thus a much stronger interaction with the environment, compared to the $4f$ case. As a consequence, the $5f$ electrons in actinides are, as a rule, delocalized due to their participation in bonding, and hence there is considerable hybridization of the $5f$ states with the valence states of neighboring atoms ($5f$-ligand hybridization) in the crystal lattice. Consequently, the magnetic moments due to the itinerant $5f$ electrons are much smaller than expected for a free U^{3+} or U^{4+} ion. On the other hand, the hybridization leads also to strong magnetic anisotropy of a type depending on the crystal structure. In this respect, we speak about the hybridization-induced magnetic anisotropy. The hexagonal structure of the ZrNiAl type (Fig. 1) exhibits a relatively close packing of U and transition-metal atoms within the U-T layers leading to a highly correlated electron gas within the U-T basal-plane layers. Clearly, the most important parameter concerning the two-ion ($5f$-$5f$) interaction is the U-U spacing.[16] In UNiAl, the U-U separation amounts to 344.8 pm at 40 K, a value inside the critical region (340–360 pm). In this case, also $5f$-ligand hybridization is expected to play an important role. One of the most apparent manifestations are the hybridization-induced magnetic moments on the transition-metal sites as was observed by Paixão *et al.*[14] in the case of URhAl that crystallizes in the same structure as UNiAl. Highly correlated $5f$-electron states are expected to form a band pinned at the Fermi surface. The high density of states at E_F is projected into high γ values of the low-temperature specific heat and into highly anomalous transport properties.

In the case of UNiAl, one immediately notes the strongly reduced magnitude of the U moments of $(1.24\pm0.03)\mu_B$ in agreement with expectations based on the U-U separation. Moreover, due to reasons given in the preceding paragraph (anisotropic hybridization), UNiAl exhibits a strong uniaxial magnetic anisotropy that locks the U-moment orientation along the c axis that also is the easy-magnetization direction. The anisotropy energy determined from single-crystal studies[1,2] exceeds several hundreds of tesla if derived from the high-field magnetization measurements and several hundreds of kelvin if derived from magnetic susceptibility studies.[1] With conventionally available magnetic fields the direction of U moments is hardly changed. For instance, at 4.2 K a magnetic field of 11.4 T applied along the c axis induces a moment reorientation manifest as a spin-flip transition in the magnetization curve[1] while the magnetic response in fields applied within the basal plane is much smaller, which is also true for the paramagnetic range. At 4.2 K, the magnetization curve for field applied perpendicular to the c axis is a straight line up to 35 T yielding only $0.14\mu_B$/f.u. in this field. However, we do not have any direct evidence for anisotropically induced magnetic moments on Ni sites. Our data do not indicate any sizable moments centered at Ni sites.

The participation of the electronic states of $5f$ origin in anisotropic bonding and their presence at the Fermi surface can be documented by the transport and thermal properties of UNiAl.[1] The electrical resistivity is strongly anisotropic. An anomalous $T^{5/3}$ power law is found at low temperatures for current parallel to the hexagonal axis. The rather high residual resistivities are strongly reduced upon application of a magnetic field that is high enough to force the system to order ferromagnetically. Finally, the low-temperature specific-heat coefficient in UNiAl that amounts at zero field to 167 $\mathrm{mJ/mol_U\,K^2}$ (Ref. 1) reflects a high density of states of $5f$ origin at the Fermi surface.

While the coupling of the U moments along the c axis is antiferromagnetic in UNiAl, the coupling within the basal plane is in principle ferromagnetic albeit a sine-wave modulation of U moments within the basal plane is found. In this respect, UNiAl is unique among the UTX compounds crystallizing in the ZrNiAl type of structure because all other compounds consist of ferromagnetic basal-plane sheets coupled in various ways along the c axis.[2] The uniqueness of UNiAl is reflected also by the fact that the U moments are not equal at all sites. First, the three U sites, which are crystallographically equivalent, do not carry the same moment within the crystallographic unit cell. Second, the modulation is not even partially squared-up down to the lowest temperature applied in the experiment (1.7 K). Moreover, the propagation vector $\mathbf{q}=\pm(0.1,0.1,0.5)$ is invariant with temperature. This observation is striking because, normally, equal-moment structures are found in the ground state due to minimum magnetic entropy. In the case of sine-wave modulated structures one usually observes a temperature dependence of the propagation vector. This is not the case in UNiAl and, at this moment, we do not have a clear explanation for this behavior.

In conclusion, we have reported on the antiferromagnetic structure of UNiAl. The compound crystallizes in the hexagonal ZrNiAl-type structure. Below $T_N=19.3$ K, UNiAl orders antiferromagnetically with propagation vector $\mathbf{q}=(0.1,0.1,0.5)$. The magnetism in UNiAl is due to U moments that are oriented along the hexagonal axis and modulated sinusoidally within the basal plane. The maximum size of the U moment is $(1.24\pm0.03)\mu_B$/U. However, the three U atoms that are crystallographically equivalent do not carry the same moment within the crystallographic unit cell. The propagation vector of the antiferromagnetic structure does not change in the whole temperature range of existence of

this structure. Antiferromagnetic correlations that propagate also with $\mathbf{q}=(0.1,0.1,0.5)$ can be traced at temperatures up to 30 K.

ACKNOWLEDGMENTS

This work is part of the research program of the Stichting voor Fundamenteel Onderzoek der Materie (FOM), which is financially supported by the Nederlandse Organisatie voor Wetenschappelijk Onderzoek (NWO). Support to K.P., P.J., M.O., and V.S. at CENG, Grenoble given in the framework of the E.C. funded program PECO is acknowledged. The work of V.S. was also partly supported by the Grant Agency of the Czech Republic (Grant No. 40/97). The work of K.P. was partly sponsored also by Japanese Society for Promotion of Science (JSPS).

*Author to whom all correspondence should be addressed. Present address: Department of Physics, Faculty of Science, Hiroshima University, Kagamiyama 1-3-1, Higashi-Hiroshima 739, Japan; Fax: +81 824 24 0716, electronic address: prokes@butsuri.sci.hiroshima-u.ac.ip. Also at Department of Metal Physics, Charles University, Ke Karlovu 5, 121 16 Prague 2, The Czech Republic.

†Also at Department of Metal Physics, Charles University, Ke Karlovu 5, 121 16 Prague 2, The Czech Republic.

[1] E. Brück, H. Nakotte, F. R. de Boer, P. F. de Châtel, H. P. van der Meulen, J. J. M. Franse, A. A. Menovsky, N. H. Kim-Ngan, L. Havela, V. Sechovský, J. A. A. J. Perenboom, N. C. Tuan, and J. Šebek, Phys. Rev. B **49**, 8852 (1994).

[2] V. Sechovský and L. Havela, in *Ferromagnetic Materials*, edited by E. P. Wohlfarth and K. H. J. Buschow (North-Holland, Amsterdam, 1988), Vol. 4, p. 309.

[3] M. Diviš, M. Olšovec, M. Richter, and H. Eschrig, J. Magn. Magn. Mater. **140-144**, 1365 (1994).

[4] J. M. Fournier and P. Burlet, in *Proceedings of the 21ièmes Journées des Actinides, Montechoro, 1991*, edited by N. Marques and A. P. Matos (ICEN-LNETI, Sacavem, 1991), p. 2.3.

[5] H. Maletta, R. A. Robinson, A. C. Lawson, V. Sechovský, L. Havela, L. Jirman, M. Diviš, E. Brück, F. R. de Boer, A. V. Andreev, K. H. J. Buschow, and P. Burlet, J. Magn. Magn. Mater. **105-107**, 21 (1992).

[6] M. S. Lehman and F. K. Larsen, Acta Crystallogr., Sect. A: Cryst. Phys., Diffr., Theor. Gen. Crystallogr. **31**, 245 (1974).

[7] A. C. Larson and R. B. von Dreele, Los Alamos National Laboratory Report No. LA-UR-86-748, 1992 (unpublished).

[8] J. Rodrigues-Carvajal, computer code FULLPROF, Version 3.2, 1997.

[9] V. F. Sears, Neutron News **3**, 26 (1992).

[10] A. J. Freeman, J. P. Desclaux, G. H. Lander, and J. Faber, Phys. Rev. B **13**, 1168 (1976).

[11] P. J. Becker and P. Coppens, Acta Crystallogr., Sect. A: Cryst. Phys., Diffr., Theor. Gen. Crystallogr. **30**, 129 (1974); **30**, 148 (1974); **31**, 417 (1975).

[12] E. F. Bertaut, Acta Crystallogr., Sect. A: Cryst. Phys., Diffr., Theor. Gen. Crystallogr. **24**, 217 (1968).

[13] P. Javorský, N. C. Tuan, M. Diviš, L. Havela, P. Svoboda, V. Sechovský, and G. Hilscher, J. Magn. Magn. Mater. **140-144**, 1139 (1995).

[14] J. A. Paixão, G. H. Lander, P. Brown, H. Nakotte, F. R. de Boer, and E. Brück, J. Phys.: Condens. Matter **4**, 829 (1992); J. A. Paixão, G. H. Lander, A. Delapalme, H. Nakotte, F. R. de Boer, and E. Brück, Europhys. Lett. **24**, 607 (1993).

[15] J. Rossat-Mignod, in *Methods of Experimental Physics*, edited by K. Sköld and D. L. Price (Academic, New York, 1987), Vol. 23, P. C, p. 69, and references therein.

[16] H. H. Hill, in *Plutonium 1970 and Other Actinides*, edited by W. N. Miner (AIME, New York, 1970), p. 1.